

indicate that the systemic infection of 5-58 resulted from recombination between mRNA expressed by the plant and the challenging deletion inoculum.

Several deletions within 5-58 shifted the capsid open reading frame (ORF) 13 codons (Fig. 3). Despite these amino acid substitutions, sap extracts from 5-58 initiated typical CCMV systemic infections in both cowpeas and *N. benthamiana*, and normal yields of virion RNA were recovered from both species. Therefore, RNA recombination in 5-58 produced a mutant form of CCMV by aberrant homologous recombination within the overlapping region of the transgenic mRNA and the viral inoculum.

Of 125 transgenic plants tested, four recombinant viruses have been verified from three different transgenic plant lines. Despite attempts to favor homologous recombination by providing 338 overlapping nucleotides between the transgenic viral mRNA and genomic RNA of the challenging virus, sequences derived from recombinants revealed that each resulted from a distinctly different aberrant homologous recombination event (Fig. 3). Therefore, precise recombination was not required to restore virus viability.

Previous bromovirus studies have demonstrated RNA recombination only within noncoding regions (4-6). This report demonstrates intragenic recombination in 3% of the transgenic plants inoculated. Regeneration of a functional ORF must provide stringent selection pressure on recombination products.

One factor that may contribute to recombination is the presence of the complete 3' untranslated sequence from CCMV RNA3 in the mRNA transcript. Since the viral replicase complex initiates minus strand RNA synthesis on this terminal sequence (20), its presence may enable replication to begin on the mRNA transcript and then switch to the RNA inoculum to complete synthesis. Thus, the presence of 3' untranslated sequence may target the transcript to the replication complex and enhance the possibility of recombination. This would be consistent with the template-switching model for RNA replication (21). Because the 3' untranslated region of the virus may lend stability to the viral RNA, it is frequently included in transgenic constructions.

Recombination during RNA virus replication contributes to the rapid evolution of RNA viruses and could affect host range or vector specificity, traits that have been attributed to capsid proteins of several plant viruses (22). As transgenically expressed viral mRNA is available to recombine with replicating RNA viruses, RNA recombina-

tion should be considered when analyzing the risks posed by virus-resistant transgenic plants.

## REFERENCES AND NOTES

- M. M. C. Lai, *Microbiol. Rev.* **56**, 61 (1992).
- J. Burgyan, F. Grieco, M. Russo, *J. Gen. Virol.* **70**, 235 (1989); B. I. Hillman, J. C. Carrington, T. J. Morris, *Cell* **51**, 427 (1987).
- G. C. Angenent, E. Posthumus, F. T. Brederode, J. F. Bol, *Virology* **171**, 271 (1989); D. J. Robinson, W. D. O. Hamilton, B. D. Harrison, D. C. Baulcombe, *J. Gen. Virol.* **68**, 2551 (1987).
- J. J. Bujarski and P. Kaesberg, *Nature* **321**, 528 (1986); A. L. N. Rao, B. P. Sullivan, T. C. Hall, *J. Gen. Virol.* **71**, 1403 (1990).
- A. L. N. Rao and T. C. Hall, *J. Virol.* **67**, 969 (1993).
- R. F. Allison, C. Thompson, P. Ahlquist, *Proc. Natl. Acad. Sci. U.S.A.* **87**, 1820 (1990).
- P. D. Nagy and J. J. Bujarski, *J. Virol.* **66**, 6824 (1992); *Proc. Natl. Acad. Sci. U.S.A.* **90**, 6390 (1993).
- P. J. Cascone, T. F. Haydar, A. E. Simon, *Science* **260**, 801 (1993).
- M. Mayo and C. Jolly, *J. Gen. Virol.* **72**, 2591 (1991).
- S. Lommel and Z. Xiong, *J. Cell Biochem.* **15A**, 151 (1991).
- R. N. Beachy, S. Loesch-Fries, N. E. Tumer, *Annu. Rev. Phytopathol.* **28**, 451 (1990).
- R. Grumet, *Hortscience* **25**, 508 (1990).
- R. E. F. Matthews, *Plant Virology* (Academic Press, San Diego, ed. 3, 1991), p. 376.
- G. A. de Zoeten, *Phytopathology* **81**, 585 (1991).
- R. F. Allison, M. Janda, P. Ahlquist, *J. Virol.* **62**, 3581 (1988).
- To avoid potential spurious mutations, we substituted a 359-base pair (bp) Sac II-Xba I fragment containing the introduced mutations for the similar fragment in the original plasmid, pCC3TP4, to form pCC3AG1. The fidelity of all constructs was confirmed by sequence analysis.
- Effects of mutations on virus infectivity were ascertained by inoculation of both cowpea, *Vigna sinensis* (Torner) Savi, and *Nicotiana benthamiana* (Domin) with full-length plasmid-derived transcripts of WT CCMV RNAs 1 and 2 and either WT RNA 3 or pCC3AG1, referred to hereafter as C1, C2, C3, and AG1. Plants became systemically infected within 14 days, and no differences were observed in either the quantity or stability of recovered virions or viral RNA.
- G. An, P. R. Ebert, A. Mitra, S. B. Ha, *Plant Mol. Biol.* **A3**, 1 (1988).
- This placed the CCMV sequence under the control of the constitutive 35S promoter and within the T-DNA region of pGA643. The pGAC-CMV plasmid was introduced by tri-parental mating into *Agrobacterium tumefaciens* strain LBA4404 for use in leaf disk transformation of *N. benthamiana*. Transformed explants were selected for kanamycin resistance in tissue culture.
- W. Miller, J. Bujarski, T. Dreher, T. Hall, *J. Mol. Biol.* **187**, 537 (1986).
- K. Kirkegaard and D. Baltimore, *Cell* **47**, 433 (1986).
- W. Dawson and M. Hilf, *Annu. Rev. Plant Physiol. Plant Mol. Biol.* **43**, 527 (1992).
- R. F. Allison, M. Janda, P. Ahlquist, *Virology* **172**, 321 (1989).
- Single-letter abbreviations for amino acid residues are as follows: A, Ala; C, Cys; D, Asp; E, Glu; F, Phe; G, Gly; H, His; I, Ile; K, Lys; L, Leu; M, Met; N, Asn; P, Pro; Q, Gln; R, Arg; S, Ser; T, Thr; V, Val; W, Trp; and Y, Tyr.
- Supported by the Consortium for Biotechnology Research Inc., Monsanto Company, St. Louis, MO, and Michigan Agricultural Experimentation Station.

8 October 1993; accepted 27 January 1994

## High-Resolution Molecular Discrimination by RNA

Robert D. Jenison, Stanley C. Gill, Arthur Pardi, Barry Polisky\*

Species of RNA that bind with high affinity and specificity to the bronchodilator theophylline were identified by selection from an oligonucleotide library. One RNA molecule binds to theophylline with a dissociation constant  $K_d$  of 0.1  $\mu$ M. This binding affinity is 10,000-fold greater than the RNA molecule's affinity for caffeine, which differs from theophylline only by a methyl group at nitrogen atom N-7. Analysis by nuclear magnetic resonance indicates that this RNA molecule undergoes a significant change in its conformation or dynamics upon theophylline binding. Binding studies of compounds chemically related to theophylline have revealed structural features required for the observed binding specificity. These results demonstrate the ability of RNA molecules to exhibit an extremely high degree of ligand recognition and discrimination.

The conformational complexity of libraries of random-sequence single-stranded oligonucleotides offers the opportunity to search for molecules that show high-affinity binding to biomedically important targets (1). A procedure called SELEX (systematic evolution of ligands by exponential enrichment) permits the iterative isolation and amplification of RNA or DNA oligonucleotides with selective affinity for defined

targets, which represents a route to drug discovery (1). With this technique, RNA oligomers have been isolated that have high affinity and specificity for a variety of both protein and small molecule targets, including bacteriophage T4 DNA polymerase (1), R17 coat protein (2), human immunodeficiency virus (HIV) reverse transcriptase (3), HIV Rev protein (4), basic fibroblast growth factor (5), adenosine triphosphate (6), and several amino acids (7). Oligomers of DNA that recognize thrombin (8) and oligomers of RNA and DNA that bind to organic dyes (9) have also been identified.

Many of these SELEX-generated oligo-

R. D. Jenison, S. C. Gill, B. Polisky, NeXagen, Inc., 2860 Wilderness Place, Boulder, CO 80301, USA.  
A. Pardi, Department of Chemistry and Biochemistry, University of Colorado, Boulder, CO 80309, USA.

\*To whom correspondence should be addressed.

mers were targeted to proteins that bind polyanions, such as nucleic acids or heparin. However, SELEX has the potential to identify high-affinity ligands to a much wider variety of molecular targets. Our study was designed to identify short oligo-

nucleotides that bind with extremely high affinity to the small molecule target theophylline and also have high levels of molecular discrimination against caffeine, which differs from theophylline by a single methyl group at the N-7 position.

Theophylline is a naturally occurring alkaloid that is used widely as a bronchodilator in the treatment of asthma, bronchitis, and emphysema (10). Because of its narrow therapeutic index, serum levels must be monitored carefully to avoid serious toxicity (10). Theophylline is also chemically similar to theobromine (3,7-dimethylxanthine), which, like caffeine, is present in serum samples. Thus, diagnostic methods must discriminate efficiently among these compounds (11).

To screen for RNA molecules with affinity for theophylline, we generated a pool of  $10^{14}$  RNA molecules that contain a 40-nucleotide region of random sequence. The RNA pool was added to a Sepharose column to which 1-carboxypropyl (CP) theophylline was covalently cross-linked (12). Bound RNA was eluted by the addition of 0.1 M theophylline. The eluted RNA was converted to DNA and amplified by polymerase chain reaction (PCR) as described (13). This set of procedures constituted one SELEX round.

The progress of the experiment over eight rounds was monitored by determining the percent of the labeled RNA that was eluted from the column specifically by theo-

## A

### CLASS I

```

region 1                      region 2 *
TCT8-6,9  5' gagaaAUACCAgugacaacucucgagaucaCCUUGGAAG 3'
TCT8-5    AUACCAucguguaagcaagagcacgaCCUUGGCAGugugug
TCT8-1,10 gAUACCAacagcauau----uugcuguCCUUGGAAGcaacgaga
TCT8-4,8  gugAUACCAgcaucguc----uugaugcCCUUGGCAGcacuua
TCT8-7    uugucgaaucgAUACCAgcaau-----gcagcCCUUGGAAGcag
TR8-14    gAUACCAacggcauau----uugcuguCCUUGGAAGcaacuaa
TR8-8     cucucgaaAUACCAacuacucucaca----auaguCCUUGGAAG
TR8-5     uucaugucgcuugAUACCAucaaca-----augaCCUUGGAAGca

```

### CLASS II

```

region 2 *                      region 1
TCT8-3    5' ugacucgaacCCUUGGAAGaccugagu-----acagguAUACCAg 3'
TCT8-11   uCCUUGGAAGcgg-----uacggAUACCAauugaguggccauaug
TR8-28    uaucgaguggCCUUGGCAGaccaggc-----ccggAUACCAcca
TR8-29    cgagauucaCCUUGGAAGucaau-----cgugaAUACCAauuguu
TR8-9     ucagaaCCUUGGAAGcacugaauaagaucaguugAUACCA

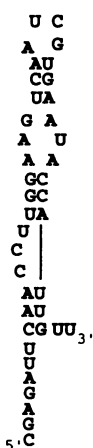
```

## B

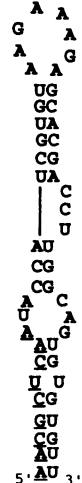
TR8-28



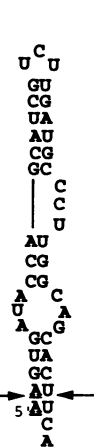
TR8-29



TCT8-5



TCT8-4



## C

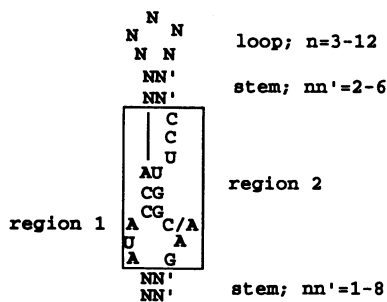


**Fig. 1. (A)** Aligned sequences for two classes of RNA molecules with affinity for theophylline. The clone number from which the sequence was derived is shown at the left of the sequence. In some cases, multiple isolates were obtained. Sequences shown comprised the 40-nucleotide sequence that was initially random at the start of the SELEX process. The conserved sequences are highlighted in upper case and provide the basis for the alignment. The arrows overlay regions of potential base complementarity. The asterisk marks the single position in region 2 that shows variability. Dashes represent absence of a nucleotide. Class I and II are related by circular permutation. **(B)** Potential secondary structures for theophylline-binding RNA species. Underlined bases were present in either the fixed 5' or 3' regions that flanked the random region. Either fixed region can contribute to the proposed structure. The arrows in the TCT8-4 ligand mark the termini of the truncated mTCT8-4, except that the AU base pair above the arrows was changed to a GC base pair in mTCT8-4. **(C)** Consensus secondary structure of theophylline-binding RNA species. The N and N' signify any complementary base pair. The numbers to the right of the structure represent the size range of the various domains observed in the sequenced RNAs. The conserved theophylline-binding region is boxed.

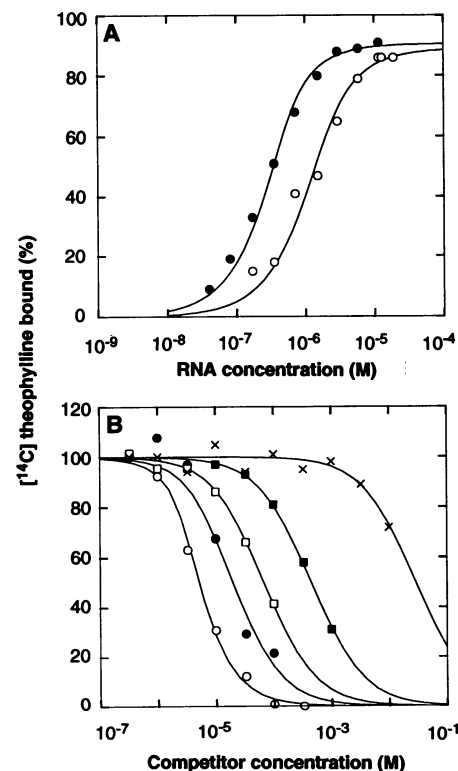


**Fig. 2. (A)** The binding of (○) TCT8-4 and (●) mTCT8-4 RNAs to theophylline (19). **(B)** Competition binding analysis of xanthine derivatives with TCT8-4 RNA (20). Competitors: (○) theophylline, (●) 3-methylxanthine, (□) xanthine, (■) hypoxanthine, and (×) caffeine. These data were used to determine competitor dissociation constants  $K_d(c)$ .

phylline. Only 0.05% of the random RNA in the first round was eluted from the column. After eight rounds, 62% of the input RNA was eluted by theophylline; this pool was designated TR8.

We diverged from this protocol after the fifth round and used a different elution protocol to increase the stringency of the selection process. Rather than eluting with theophylline immediately after washing, bound RNAs were first eluted with 0.1 M caffeine. Remaining RNAs were eluted with 0.1 M theophylline. This approach was designated "counter-SELEX." In the first counter-SELEX round, 99.7% of the

theophylline-bound RNA was eluted with caffeine. The remaining 0.3% was eluted by theophylline and amplified. By the third and final round, ~80% of this RNA pool (termed TCT8) had bound to the theophylline column.

Sequence analysis was carried out on double-strand complementary DNA populations derived from the TCT8 and TR8 pools (Fig. 1A). The sequences were split into two classes (designated I and II) that are related through circular permutation. Region 1, 5'-AUACCA-3', is completely conserved, and region 2, 5'-CCUUGG(C/A)AG-3', is completely conserved at eight

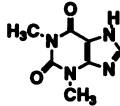
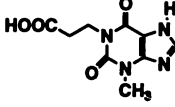
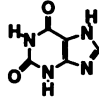
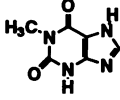
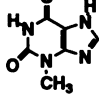
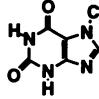
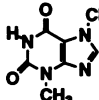
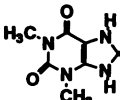
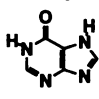
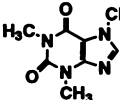
of the nine positions. The spacing between regions 1 and 2 is variable among the ligands, ranging from 8 to 20 residues.

It is possible to fold all of the TCT8 and TR8 RNAs into a similar secondary structure (Fig. 1B). Several features of these structures are notable, including a conserved CCU bulge on one side of a conserved 3-base pair stem. In addition, each RNA contains a highly conserved 6-nucleotide symmetric internal loop flanking the conserved 3-base pair stem. Sequence variations outside of this region are frequent and indicate that other nucleotides do not play a direct role in binding theophylline. A consensus secondary structure for the theophylline-binding RNA family is shown in Fig. 1C.

The binding properties of specific RNAs derived from the theophylline SELEX experiments were determined by equilibrium filtration analysis with [<sup>14</sup>C]theophylline. The values of  $K_d$  for 10 TCT8 RNAs ranged from 0.5 to 3.0  $\mu\text{M}$ . The TCT8-4 RNA ( $K_d = 0.6 \mu\text{M}$ ) was chosen for further study (Fig. 2). This binding affinity is similar to that observed for monoclonal antibodies raised against theophylline (14). No significant binding of theophylline to this RNA was observed in the absence of  $\text{Mg}^{2+}$ , but binding was constant in the presence of 5 to 100 mM  $\text{Mg}^{2+}$ .

A 38-nucleotide truncated version of the TCT8-4 RNA (mTCT8-4) (Fig. 1B) was synthesized to determine the minimum requirements for high-affinity binding to theophylline. This RNA has a  $K_d$  of 0.1  $\mu\text{M}$  for its interaction with theophylline (Fig. 2), confirming that all structural determinants required for theophylline binding are contained in this truncated RNA. Thermal denaturation studies on mTCT8-4 yielded a  $T_m$  (temperature at which 50% of the RNA is denatured) of 72°C, in the presence or absence of theophylline, indicating that this RNA forms a very stable secondary structure.

**Table 1.** Competition binding analysis with TCT8-4 RNA. The chemical structures are shown for a series of derivatives used in competitive binding experiments with TCT8-4 RNA (Fig. 2) (20). The right column represents the affinity of the competitor relative to theophylline,  $K_d(c)/K_d(t)$ , where  $K_d(c)$  is the individual competitor dissociation constant and  $K_d(t)$  is the competitive dissociation constant of theophylline. Certain data (denoted by >) are minimum values that were limited by the solubility of the competitor. Each experiment was carried out in duplicate. The average error is shown.

Compound	Structure	$K_d(c)$ ( $\mu\text{M}$ )	$K_d(c)/K_d(t)$
Theophylline		$0.32 \pm 0.13$	1
CP-theophylline		$0.93 \pm 0.20$	2.9
Xanthine		$8.5 \pm 0.40$	27
1-Methylxanthine		$9.0 \pm 0.30$	28
3-Methylxanthine		$2.0 \pm 0.7$	6.3
7-Methylxanthine		> 500	>1500
3,7-Dimethylxanthine		> 500	> 1500
1,3-Dimethyluric acid		> 1000	>3100
Hypoxanthine		$49 \pm 10$	153
Caffeine		$3500 \pm 1500$	10,900

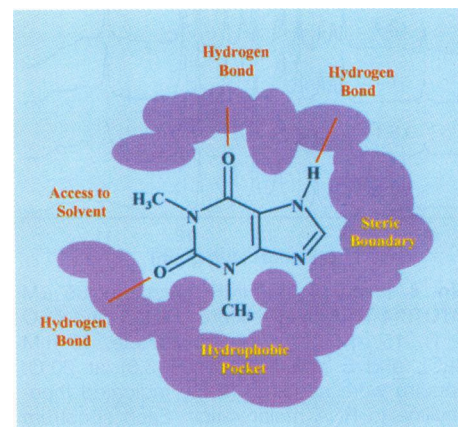


**Fig. 3.** Schematic representation of the RNA (purple) binding site for theophylline (blue).

A critical feature of a clinically useful theophylline diagnostic is distinction among closely related compounds such as caffeine. The TCT8-4 RNA was analyzed by competitive binding experiments. The binding affinity of this RNA for theophylline is 10,000-fold greater than that for caffeine (Fig. 2 and Table 1). Relative binding constants of eight other xanthine derivatives for the TCT8-4 RNA were determined (Table 1) and used to define the specific molecular components required for high-affinity binding to RNA.

The N-7 hydrogen of theophylline is critical for tight binding, as demonstrated by competition with caffeine, 7-methylxanthine, and 3,7-dimethylxanthine, which all have binding affinities less than 1/1500 of that of theophylline. Thus, we hypothesize that the N-7 hydrogen of theophylline forms a hydrogen bond with an acceptor in the RNA binding pocket (Fig. 3). The poor binding of derivatives containing an N-7 methyl could result from steric interference or inability to form a critical hydrogen bond. Addition of a keto oxygen at C-8 (1,3-dimethyluric acid) also disrupts binding. Possibilities for this disruption include interference with hydrogen bonding at N-7, disruption of a favorable electrostatic interaction at N-9, or steric interference. The N-3 methyl group contributes to binding as indicated by the fivefold greater affinity of 3-methylxanthine relative to xanthine. Comparison of the binding affinities of theophylline and CP-theophylline relative to 3-methylxanthine suggests that a carbon atom linked to N-1 contributes to RNA binding. Finally, xanthine binds with an affinity about sixfold greater than that of hypoxanthine, indicating that the C-2 keto oxygen is also important in recognition. These data are consistent with a theophylline:RNA complex that possesses a hydro-

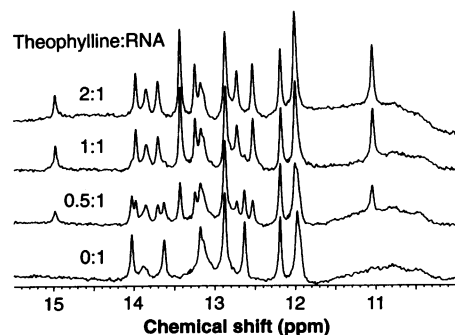


**Fig. 4.** Imino proton NMR spectra of 65  $\mu\text{M}$  mTCT8-4 RNA in a mixture of  $\text{H}_2\text{O}$  and  $\text{D}_2\text{O}$  (9:1), 15 mM potassium phosphate, 10 mM NaCl, and 5 mM  $\text{MgCl}_2$  (pH 6.8) at 20°C. Spectra were acquired at the indicated theophylline to RNA molar ratios. Each spectrum was acquired with 4096 scans with a jump-return water suppression pulse sequence (21) on a Varian VXR-500S spectrometer.

gen bond involving the N-7 position on theophylline and possibly additional hydrogen bonds involving the oxygens attached at C-2 and C-6, a binding pocket involving a steric boundary at the C-8 region, and a hydrophobic region to accommodate the N-3 methyl (Fig. 3).

To support the secondary structure model (Fig. 1B), we recorded  $^1\text{H}$  nuclear magnetic resonance (NMR) spectra on the mTCT8-4 RNA. Imino proton spectra of nucleic acids yield qualitative information on secondary structure and can be used to monitor base pair formation (15). The imino proton chemical shifts of the free RNA and the theophylline:RNA complex (Fig. 4) are consistent with the secondary structure of mTCT8-4 given in Fig. 1B.

Dramatic spectral changes were observed upon theophylline binding. Many imino proton resonances shift position in the 1:1 complex of theophylline with mTCT8-4 RNA. This spectrum also contains five additional resonances not observed in the free RNA (Fig. 4). This indicates that binding of theophylline either induces a conformational change involving formation of additional base pairs not formed in the uncomplexed RNA or stabilizes a conformation that is dynamic in the uncomplexed RNA.

The data (Fig. 4) show that at a 0.5:1.0 ratio of theophylline to RNA, there is a 1:1 mixture of free and bound RNA, demonstrating that the stoichiometry of binding is one theophylline per RNA. This is confirmed by the absence of a significant difference between the spectra taken at a 1:1 and a 2:1 ratio of theophylline to RNA.

Qualitative analysis of the spectrum of the 1:1 complex shows 14 to 15 imino proton resonances between 11.8 and 14.2 parts per million (ppm), which is the region where G and U imino protons resonate in standard GC or AU base pairs or GU wobble base pairs (16). Two additional resonances are observed in the complex (but not the free RNA) at 11 and 15 ppm. The peak at 11 ppm is consistent with several possibilities, including a G or U that forms a nonstandard base pair, such as a GA or reverse Hoogsteen AU, or a non-base paired imino proton that is inaccessible to solvent (15). An imino proton resonance at 15 ppm is unusual and suggests formation of an A or C protonated imino group (17).

In combination with previous work (1-9), we have demonstrated the application of oligonucleotide library selection to a broad size range of biomolecules. An important aspect of these studies was the use of the modified procedure counter-SELEX, which was used to accelerate the rate at which specific ligands were obtained, and more importantly, to selectively remove

RNAs with affinity for targets that are structurally closely related to the target of interest. One of the selected RNAs shows binding discrimination between theophylline and caffeine that is 10-fold better than that for available antibodies (14). In addition, this RNA possesses a binding affinity to theophylline over 100-fold greater than that to other oligonucleotides that have been selected to bind to small molecule targets (6, 7). These results illustrate that small RNAs can display molecular recognition and specificity with extremely high resolution and illustrate the potential utility of oligonucleotides as diagnostic reagents.

## REFERENCES AND NOTES

1. C. Tuerk and L. Gold, *Science* **249**, 505 (1990).
2. D. Schneider, C. Tuerk, L. Gold, *J. Mol. Biol.* **228**, 862 (1992).
3. C. Tuerk, S. MacDougall, L. Gold, *Proc. Natl. Acad. Sci. U.S.A.* **89**, 6988 (1992).
4. D. P. Bartel, M. L. Zapp, M. R. Green, J. Szostak, *Cell* **67**, 529 (1991); C. Tuerk and S. MacDougall-Waugh, *Gene*, in press.
5. D. Jellinek, C. K. Lynott, D. B. Rifkin, N. Janjic, *Proc. Natl. Acad. Sci. U.S.A.* **90**, 11227 (1993).
6. M. Sasanfar and J. W. Szostak, *Nature* **364**, 550 (1993).
7. M. Famulok and J. W. Szostak, *J. Am. Chem. Soc.* **114**, 3990 (1992); G. J. Connell, M. Illangsekare, M. Yarus, *Biochemistry* **32**, 5497 (1993).
8. L. Bock, L. Griffin, J. Latham, E. Vermaas, J. Toole, *Nature* **355**, 564 (1992).
9. A. Ellington and J. Szostak, *ibid.* **346**, 818 (1990); *ibid.* **355**, 850 (1992).
10. L. Hendeles and M. Weinberger, *Pharmacotherapy* **3**, 2 (1983).
11. M. E. Jolley *et al.*, *Clin. Chem.* **27**, 1575 (1981); L. A. Brossard, *ibid.*, p. 1931; T. Reinecke, D. Seger, R. Wears, *Ann. Emerg. Med.* **15**, 147 (1986).
12. We coupled 20 mg of CP derivatives of theophylline to 5 ml of EAH Sepharose (Pharmacia), with 60 mg of *N*-hydroxysuccinimide and 190 mg of 1-ethyl-3-(3-dimethylaminopropyl) carbodiimide in a 5-ml 1:1 mixture of dioxane and phosphate-buffered saline (pH 7.2). Reactions were performed overnight at room temperature. Coupling efficiencies were 75% for CP-theophylline, corresponding to concentrations on the column of 0.41  $\mu\text{mol/ml}$ , as determined by reaction with 2,4,6-trinitrobenzene sulfonic acid [G. Antoni *et al.*, *Anal. Biochem.* **129**, 60 (1983)].
13. The RNAs were generated by *in vitro* transcriptions with T7 RNA polymerase as previously described (1). Theophylline column material (100  $\mu\text{l}$ ) was equilibrated with 50 column volumes of buffer A [100 mM Hepes (pH 7.3), 5 mM  $\text{MgCl}_2$ , and 0.5 M NaCl], and 0.5 to 2 nmol of [ $^{32}\text{P}$ ]RNA in buffer A was applied and allowed to interact for 20 min at room temperature. The column was then washed with buffer A until eluted radioactivity was within twofold of background levels. After the wash step, 400  $\mu\text{l}$  of buffer A containing 0.1 M theophylline or caffeine was applied and incubated for 1 hour at room temperature. The column was washed with buffer A until eluted radioactivity was at background levels. The RNA-containing eluate was ethanol precipitated in the presence of 20  $\mu\text{g}$  of tRNA (Boehringer), resuspended in water, and amplified by reverse transcriptase and PCR by standard procedures (1).
14. S. M. Poncelet *et al.*, *J. Immunoassay* **11**, 77 (1990).
15. F. J. M. van de Ven and C. W. Hilbers, *Eur. J. Biochem.* **178**, 1 (1988).
16. G. Varani and I. Tinoco Jr., *Q. Rev. Biophys.* **24**, 479 (1991).
17. V. Sklenar and J. Feigon, *Nature* **345**, 836 (1990).

18. S. C. Gill, S. E. Weitzel, P. H. von Hippel, *J. Mol. Biol.* **220**, 307 (1991).
19. A rapid procedure called "equilibrium filtration" was developed to assess theophylline binding by oligonucleotides. These assays were performed by the addition of [ $^{14}\text{C}$ ]theophylline and RNA at indicated concentrations to a 150- $\mu\text{l}$  reaction mixture containing 100 mM Hepes (pH 7.3), 5 mM  $\text{MgCl}_2$ , and 50 mM NaCl. Each binding mixture was incubated for 5 min at 25°C. The mixture was then placed in a Microcon 10 filtration device (Amicon) and centrifuged for 4 min at 13,000g, allowing 40  $\mu\text{l}$  of solution to flow through the membrane. Similar to equilibrium dialysis, the solution that remained above the molecular-weight cutoff membrane contains free theophylline, free RNA, and RNA-bound theophylline, and the filtrate contains only free theophylline at an equivalent concentration to the free theophylline in the initial solution. A 25- $\mu\text{l}$  sample was removed from each side of the filter, and the radioactivity was determined by scintillation counting. Bound theophylline was determined by the difference between the theophylline concentration of the filtrate and the theophylline concentration of the retentate. Data were fit by a least squares analysis to a standard quadratic binding equation (18) for the observed 1:1 stoichiometry. Equilibrium dialysis was also used to measure binding of theophylline and yielded dissociation constants within a factor of 2 of those obtained by equilibrium filtration.
20. Equilibrium filtration assays were performed by the addition of various concentrations of the potential competitor to 1  $\mu\text{M}$  [ $^{14}\text{C}$ ]theophylline and 3.3  $\mu\text{M}$  TCT8-4 RNA in a 150- $\mu\text{l}$  reaction mixture containing 100 mM Hepes (pH 7.3), 5 mM  $\text{MgCl}_2$ , and 50 mM NaCl. Competition data were fit by a standard competition equation and fitting procedure (18) with a 1:1 stoichiometry of competitor to RNA. A  $K_d$  of 0.45  $\mu\text{M}$  for theophylline binding to RNA was used.
21. P. Plateau and M. Gueron, *J. Am. Chem. Soc.* **104**, 731 (1982).
22. We thank C. Tuerk, D. Zichi, D. Parma, N. Janjic, D. McGee, W. Pieken, B. Eaton, K. Yamamoto, and L. Gold for thoughtful comments on this work and D. Bridon for synthesis of theophylline compounds. This work was partially supported by NIH grant AI33098 and an NIH Research Career Development Award (AI01051) to A.P. The 500-MHz NMR spectrometer was purchased with partial support from NIH grant RR03283. A.P. also thanks the W. M. Keck Foundation for their generous support of RNA science on the Boulder campus.

6 December 1993; accepted 24 January 1994

## Channel-Like Function of the Na,K Pump Probed at Microsecond Resolution in Giant Membrane Patches

Donald W. Hilgemann

Ion transporters can be thought of as ion channels that open and close only at one end at a time. As in real channels, ions may cross through an electrical field as they diffuse into and bind within the transporter pore, thereby generating electrical current. Extracellular sodium binding by the sodium potassium (Na,K) pump is associated with ultrafast charge movements in giant cardiac membrane patches. The charge movements are complete within 4 microseconds. They occur only when binding sites are open to the extracellular side, and they are abolished by ouabain and by the removal of extracellular sodium. Fast extracellular ion binding may be the exclusive source of Na,K pump electrogenicity.

The adenosine triphosphate (ATP)-driven Na,K pump, or Na,K adenosine triphosphatase, extrudes three Na ions in exchange for two K ions and therefore generates an electrical current (1) (Fig. 1A). Recently, it was proposed that the immediate source of electrogenicity in the Na,K pump cycle is the binding and dissociation of Na from an "access channel" open to the extracellular side (2) (step 4 of Fig. 1A). This proposal explains neatly why changes of extracellular Na and membrane potential appear equivalent in Na flux studies (2) and why extracellular Na inhibits pump activity in a voltage-dependent manner (3, 4). However, important kinetic predictions have not been verified. Most importantly, when binding sites are open to the extracellular side ("E<sub>2</sub>" conformation), it should be possible to record ultrafast charge movements related to Na binding and dissociation. Similar proposals and considerations apply equally to a number of other transporters (5).

The giant cardiac membrane patch technique (6) is well suited to test such predictions, because it allows a fast (4  $\mu\text{s}$ ) voltage clamp of a large membrane area ( $\sim 10$  pF) with  $\sim 1000$  Na,K pump sites per square micrometer. To facilitate both the identifi-

cation and quantification of fast charge movements, charge transfer per se is recorded directly through an integrating patch-clamp amplifier. The charge transfer signals thus represent the time integral of membrane current, and membrane current is their first derivative. The protocols used may be derived from Fig. 1A, which illustrates the simplest possible access-channel model of the Na,K pump; Fig. 1B illustrates a refined model of Na release that will be outlined with experimental results.

The charge movements (7) are recorded in the absence of K to prevent pump cycling (that is, steps 5 to 8 in Fig. 1A). In the additional absence of cytoplasmic Na and ATP, the pump orients to a configuration with empty binding sites open to the cytoplasmic side ("E<sub>1</sub>" conformation). Voltage pulses are first applied under this base line condition, whereby transitions to the other illustrated pump states are not possible. Either Na or ATP can be applied individually to the cytoplasmic side without any clear changes of base line signals, indicating that cytoplasmic Na binding (step 1) is not strongly electrogenic (8, 9). When Na and ATP are applied together, however, the pump is phosphorylated and the transporter pore closes from the cytoplasmic side, thereby "occluding" Na within the pump (step 2). The subsequent reactions (steps 3 and 4)

include electrogenic steps (9), and they can then be driven back and forth by changes of membrane potential (dotted field). The corresponding charge movements (3, 10) are isolated by the subtraction of records in the absence of cytoplasmic Na, ATP, or both from records in the presence of cytoplasmic Na and ATP (11).

Typical Na,K pump charge movements are shown in Fig. 2A, with the use of voltage steps from 0 mV to the different indicated potentials ( $-250$  to  $+150$  mV in 50-mV intervals; 10 mM cytoplasmic Na, 120 mM extracellular Na, no other monovalent cations, 0.4 mM ATP) with subtraction of the base line signals without ATP (12). Slow components over 2 to 6 ms ( $Q_{\text{slow}}$ ) dominate the records, and fast components ( $Q_{\text{fast}}$ ) appear as initial charge jumps in the first 100  $\mu\text{s}$  during voltage steps. The  $Q_{\text{slow}}$  components can all be fitted to single exponential functions that are plotted with each record as a dashed line. The exponentials are hardly visible outside signal noise, suggesting that the time course of individual  $Q_{\text{slow}}$  components may be determined by a single reaction. The rate constants of  $Q_{\text{slow}}$  ("k<sub>slow</sub>"; Fig. 2B) decrease to a minimum at positive potentials [as in (3, 10)],  $\sim 400$  s<sup>-1</sup> in these records at 37°C. They appear to saturate toward a maximal value with hyperpolarization, and their voltage dependence can be described by a Boltzmann function (midpoint,  $-170$  mV; slope, 0.74, appropriate for movement of one charge through 74% of the membrane field). Complete saturation at negative potentials was found when the initial rates were examined from  $-50$  to  $-400$  mV during 0.4-ms voltage pulses. The rate of  $Q_{\text{slow}}$  (as well as its magnitude) already reaches a maximum value at  $-150$  mV when extracellular Na is increased to 180 mM.

The fact that the reaction rates of  $Q_{\text{slow}}$  saturate at both extremes of potential and are dependent on extracellular Na suggests that a fast, electrogenic Na binding reaction may be "sandwiched" between (that is,

Department of Physiology, University of Texas Southwestern Medical Center at Dallas, 5323 Harry Hines Boulevard, Dallas, TX 75235, USA.